



Simultaneous determination of catecholamines, uric acid and ascorbic acid at physiological levels using poly(*N*-methylpyrrole)/Pd-nanoclusters sensor

Nada F. Atta *, Maher F. El-Kady, Ahmed Galal

Department of Chemistry, Faculty of Science, University of Cairo, Giza 12613, Egypt

ARTICLE INFO

Article history:

Received 2 October 2009

Received in revised form 17 December 2009

Accepted 6 January 2010

Available online 11 January 2010

Keywords:

Pd nanoclusters

Electrochemical sensor

Poly(*N*-methylpyrrole)

Catecholamine neurotransmitters

Ascorbic acid

Uric acid

ABSTRACT

An interesting electrochemical sensor has been constructed by the electrodeposition of palladium nanoclusters (Pd_{nano}) on poly(*N*-methylpyrrole) (PMPy) film-coated platinum (Pt) electrode. Cyclic voltammetry, electrochemical impedance spectroscopy (EIS), and scanning electron microscopy were used to characterize the properties of the modified electrode. It was demonstrated that the electroactivity of the modified electrode depends strongly on the electrosynthesis conditions of the PMPy film and Pd_{nano}. Moreover, the modified electrode exhibits strong electrocatalytic activity toward the oxidation of a mixture of dopamine (DA), ascorbic acid (AA), and uric acid (UA) with obvious reduction of overpotentials. The simultaneous analysis of this mixture at conventional (Pt, gold [Au], and glassy carbon) electrodes usually struggles. However, three well-resolved oxidation peaks for AA, DA, and UA with large peak separations allow this modified electrode to individually or simultaneously analyze AA, DA, and UA by using differential pulse voltammetry (DPV) with good stability, sensitivity, and selectivity. This sensor is also ideal for the simultaneous analysis of AA, UA and either of epinephrine (E), norepinephrine (NE) or L-DOPA. Additionally, the sensor shows strong electrocatalytic activity towards acetaminophen (ACOP) and other organic compounds. The calibration curves for AA, DA, and UA were obtained in the ranges of 0.05 to 1 mM, 0.1 to 10 μM, and 0.5 to 20 μM, respectively. The detection limits (signal/noise [S/N] = 3) were 7 μM, 12 nM, and 27 nM for AA, DA, and UA, respectively. The practical application of the modified electrode was demonstrated by measuring the concentrations of AA, DA, and UA in injection sample, human serum, and human urine samples, respectively, with satisfactory results. The reliability and stability of the modified electrode gave a good possibility for applying the technique to routine analysis of AA, DA, and UA in clinical tests.

© 2010 Elsevier Inc. All rights reserved.

Catecholamines are a class of neurotransmitters, and their detection in the human body has been of great interest to neuroscientists. They include dopamine (DA),¹ epinephrine (E), and norepinephrine (NE) and play important roles in various biological, pharmacological, and physical processes [1]. They are widely distributed in the mammalian central nervous system for message transfer [2]. DA, ascorbic acid (AA), and uric acid (UA) are compounds of great biomedical interests, playing determining roles in human metabolism. DA is one of the crucial catecholamine neurotransmitters that

play an important role in the function of central nervous, renal, hormonal, and cardiovascular systems [3]. Thus, a loss of DA-containing neurons may lead to neurological disorders such as Parkinsonism and schizophrenia [4]. AA is present in both animal and plant kingdoms, is a vital vitamin in human diet, and is very popular for its antioxidant properties. It has been used for the prevention and treatment of common cold, mental illness, infertility, and cancer and in some clinical manifestations of human immunodeficiency virus (HIV) infections [5]. UA is the primary end product of purine metabolism. The extreme abnormalities of UA levels in the body are symptoms of several diseases, including gout, hyperuricemia, and Lesch–Nyan disease [6]. Therefore, simultaneous detection of DA, AA, and UA is a challenge of critical importance not only in the field of biomedical chemistry and neurochemistry but also for diagnostic and pathological research. However, the simultaneous determination of AA, DA, and UA at conventional solid electrodes (carbon and metal) usually struggles because they undergo an overlapping oxidation potential and electrode fouling takes place due to the adsorption of oxidation products [7]. Therefore, it is essential to develop simple and rapid methods for their determination in routine

* Corresponding author. Fax: +20 0235727556.

E-mail address: nada_fah1@yahoo.com (N.F. Atta).

¹ Abbreviations used: DA, dopamine; E, epinephrine; NE, norepinephrine; AA, ascorbic acid; UA, uric acid; HIV, human immunodeficiency virus; Ppy, polypyrrole; ssDNA, single-stranded DNA; PMPy, poly(*N*-methylpyrrole); PMPy/Pd_{nano}, PMPy modified with palladium nanoclusters; ECP, electronically conducting polymer; CV, cyclic voltammetry; Pt, platinum; DPV, differential pulse voltammetry; ACOP, acetaminophen; MPy, *N*-methylpyrrole; Bu4NPF6, tetrabutylammonium hexafluorophosphate; HPLC, high-performance liquid chromatography; EIS, electrochemical impedance spectroscopy; BE, bulk electrolysis; SEM, scanning electron microscopy; PBS, phosphate-buffered solution; Au, gold; S/N, signal/noise.

analysis without cross-interferences. Of these, electrochemical methods have received much interest because they are more selective, less expensive, and less time-consuming and can potentially be applied to a real-time determination *in vivo* [8]. There are reports of using polymer films [9], nanoparticles [10], self-assembled monolayers [11], and metal oxide [3] modified electrodes to simultaneously determine DA and AA and also in the presence of UA. All of the reported modified electrodes have their advantages and limitations.

Polypyrrole (Ppy) is one of the most extensively used conducting polymers in the design of bioanalytical sensors [12]. Versatility of this polymer is determined by a number of properties: redox activity [13], ion exchange and ion discrimination capacities [14], electrochromic effect depending on electrochemical polymerization conditions and charge/discharge processes [15], strong absorptive properties toward gases [16], proteins [17], DNA [18], catalytic activity [19], corrosion protection properties [20], and the like. Most of these properties are dependent on the synthesis procedure [21]. Ppy may be electrochemically generated and deposited on the conducting surfaces. This technique is successfully exploited for development of various types of electrochemical sensors and biosensors. In this respect, several major directions are straightforward: (i) catalytic sensors based on immobilized enzymes [22], (ii) immunosensors based on immobilized affinity exhibiting proteins [23], (iii) DNA sensors based on covalently immobilized and/or entrapped single-stranded DNA (ssDNA) [24], and (iv) affinity sensors based on molecularly imprinted polymers [25]. Nowadays, this polymer becomes one of the major tools for nanobiotechnological applications [26]. Various approaches have been considered for the synthesis of Ppy, including chemical and electrochemical methods [27]. It was reported that the catalytic activity of Ppy films depends on the synthesis conditions [21,27]. In our report, potentiostatic (controlled potential electrolysis) and potentiodynamic (cyclic voltammetry) techniques were used to synthesize poly(*N*-methylpyrrole) (PMPy) films, and their activities were tested in the electrooxidation of the compounds of study. PMPy has attracted attention as a possible alternative to PPy for technological applications in spite of its lower conductivity [28].

A step forward with respect to “simple” modification with pristine conducting polymers consists in the inclusion of metal functionalities inside the polymeric matrix to further increase the performances of the resulting composite material. In particular, inclusion of noble metal nanoparticles, whose catalytic properties are well known [20], constitutes one of the most interesting possibilities. Similar composites based on polypyrrole and polyaniline have been reported recently [29], although a precise definition of the structure and properties of the material is far from being achieved exhaustively.

Here we report the synthesis, characterization, and sensing applications of a composite material based on PMPy modified with palladium nanoclusters (PMPy/Pd_{nano}). The aim of the development of the composite material is to improve the electrocatalytic properties of the simple polymeric electrode coating. Several procedures have been employed to prepare metal-supported nanoparticles on different carbon supports and electronically conducting polymers (ECPs) [30]; of these, electrochemical deposition is an efficient method for the preparation of metal nanoparticles. It is widely used with different strategies/methodologies such as cyclic voltammetry (CV) [31], potential step deposition [32], and double pulse [33]. Among these, potential step deposition provides a tool to fine-tune the amount of metal deposited, the number of metallic sites, and their size. Various electrochemical methods have been described for the preparation of ECP/metal nanoparticles, but the most popular approach is the deposition of metal nanoparticles onto electrodes previously coated with ECP films [34]. Moreover,

the methods of formation of the polymer film and deposition of metal nanoparticles have a strong impact on the characteristics of the polymer/metal nanoparticle composites and the possible synergistic effects between the dispersed metal nanoparticles and polymer film [10–14]. For these reasons, we explored how these factors affect the composite-modified electrode.

In the current study, PMPy/Pd_{nano} composite-modified platinum (Pt) electrode was used for the simultaneous determination of catecholamines, UA, and AA. The electrochemical behaviors of these species at our modified electrode were investigated using CV and differential pulse voltammetry (DPV) techniques. Based on the different electrocatalytic activities of the modified electrode toward AA, DA, and UA, a sensitive and selective method for their simultaneous determination was established. The detection of AA in injection samples, UA in human urine, and DA in human serum was finally demonstrated as real sample applications. Furthermore, this work addresses the electrocatalytic properties of PMPy/Pd_{nano} toward the oxidation of acetaminophen (ACOP), which is commercially known as paracetamol, as well as some organic compounds. ACOP is an antipyretic and analgesic drug widely used worldwide for the relief of mild to moderate pain associated with headache, backache, arthritis, and postoperative pain. Therefore, its determination is of importance as well.

Materials and methods

Chemicals and reagents

All chemicals were used as received without further purification except *N*-methylpyrrole (MPy, distilled under rotary evaporation prior to use). MPy, tetrabutylammonium hexafluorophosphate (Bu₄NPF₆), acetonitrile (high-performance liquid chromatography [HPLC] grade), hydroquinone, catechol, DA hydrochloride, E, NE, *L*-DOPA, methyl-*L*-DOPA, *p*-aminophenol, acetaminophen, AA, UA, tryptophan, cysteine, tyrosine, tyramine, serotonin hydrochloride, glucose, sulfuric acid, sodium chloride, potassium chloride, calcium chloride, and magnesium chloride were supplied by Aldrich Chemical (Milwaukee, WI, USA). Palladium(II) chloride (Schering Kaul Paum, Berlin, Germany) was also used. Aqueous solutions were prepared using doubly distilled water.

Electrochemical cells and equipment

Electrochemical polymerization and characterization were carried out with a three-electrode/one-compartment glass cell. The working electrode was Pt disk (diameter = 1.5 mm). The auxiliary electrode was in the form of 6.0 cm Pt wire. All of the potentials in the electrochemical studies were referenced to Ag/AgCl (3.0 M NaCl) electrode. Working electrode was mechanically polished using alumina (2 μm)/water slurry until no visible scratches were observed. Prior to immersion in the cell, the electrode surface was rinsed thoroughly with distilled water and dried. Other disk electrodes were used: gold (diameter = 1.5 mm) and glassy carbon (diameter = 3 mm). All experiments were performed at 25 °C.

The electrosynthesis of the polymers and their electrochemical characterization were performed using a BAS-100B electrochemical analyzer (Bioanalytical Systems [BAS], West Lafayette, IN, USA). Electrochemical impedance spectroscopy (EIS) measurements were performed using a Gamry-750 system and a lock-in amplifier that were connected to a personal computer. The data analysis software was provided with the instrument and applied nonlinear least squares fitting with the Levenberg–Marquardt algorithm. All impedance experiments were recorded between 0.1 Hz and 100 kHz with an excitation signal of 10 mV amplitude.

A Jeol JSM-T330A instrument was used to obtain the scanning electron micrographs of the different films.

Electropolymerization of MPy

MPy was electropolymerized from a monomer solution containing 0.05 M MPy/0.05 M Bu₄NPF₆/acetonitrile using two electrochemical methods. In the first method (bulk electrolysis [BE] method), the potential applied between the Pt disk working electrode and the reference (Ag/AgCl) was held constant at +1.8 V for 30 s and the electrode is called Pt/PMPy_(BE). In the second method (CV method), the potential is changed with time, namely 50 mV s⁻¹, between two potential limits ($E_i \sim -0.1$ V and $E_f \sim +1.8$ V) for 10 cycles and the electrode is called Pt/PMPy_(CV).

For all polymer films, the thickness was controlled by the amount of charge consumed during the electropolymerization step. Therefore, assuming 100% current efficiency during the electrochemical conversion, it is possible to use the following empirical equation [35] to roughly estimate the film thickness:

$$L = m_e \cdot j \cdot t / S, \quad (1)$$

where L is the thickness (cm), m_e is the electrochemical equivalent (mg C⁻¹), j is the current density (mA cm⁻²), t is the time (s), and S is the density (g cm⁻³). The polymer film was alternatively formed using the BE and CV methods; the total charges passed were approximately 1×10^4 μ C and 0.99×10^4 μ C, respectively, and the thicknesses were calculated to be approximately 200 and 198 nm, respectively. Because 100% current efficiency might not be obtained, this represents the maximum film thickness possible and is constant in all experiments.

Preparation of PMPy/Pd_{nano} composite electrodes

The electrodeposition of Pd_{nano} on the polymer film was reported in our previous work [36]. Briefly, a polymer film is prepared by either the BE or CV method and is washed with doubly distilled water. This was followed by the electrochemical deposition of Pd_{nano} on the polymer film from a solution of 2.5 mM PdCl₂ in 0.1 M HClO₄ by applying a double potential step (method I) or a CV program (method II) to the polymer. The double potential step conditions are $E_i = -0.05$ V, $\Delta t_i = 30$ s, $E_f = +0.01$ V, and $\Delta t_f = 300$ s, and the electrode formed in this way is indicated Pt/PMPy/Pd_{nano(I)}. In the CV method, the electrode is cycled between -0.25 and $+0.65$ V at a scan rate of 50 mV s⁻¹ for 25 cycles, and the electrode formed in this way is indicated Pt/PMPy/Pd_{nano(II)}.

Furthermore, the surface coverage (Γ) of Pd_{nano} has been calculated using the following equation:

$$\Gamma = Q/nFA, \quad (2)$$

where Q is the charge, n is the number of electrons involved in the electron transfer process ($n = 2$), F is the Faraday constant, and A is the geometric area of the Pt (0.0176 cm²) [37]. The surface coverage (Γ) of Pd_{nano} was estimated by integrating the charge (Q) of cathodic peak current of Pd_{nano} at a scan rate of 0.02 V/s. The surface coverages of Pd_{nano} were approximately 5.1×10^{-9} and 5.2×10^{-9} mol cm⁻² for the electrodeposition with methods I and II, respectively.

Results and discussion

Results of electropolymerization of MPy

The charge time and current time transients obtained during the electropolymerization of MPy by the BE method (see Fig. S1a in supplementary material) indicate a slow charge transfer due

to the previously formed polymer layer that affects the subsequent formation and thickening of PMPy. (See supplementary material for details behind this conclusion.)

Repeated cyclic voltammograms (Fig. S1b) obtained during the electropolymerization of MPy show relative decay in the current of the oxidation process that is responsible for the polymer film thickening (cf. the current of the first cycle with that of the last cycle). The decrease in current reflects the insulating character of the film formed during the first few cycles as the number of scans increases. It was mentioned earlier that a disadvantage of pyrrole is the presence of available sites for coupling in the β -position of the ring during film propagation [38]. Consequently, a break in conjugation will result and a decrease in film conductivity is observed [39].

Electrochemistry of catecholamines at PMPy-modified electrodes prepared under different electrochemical conditions

It has been mentioned that the method of polymerization of Ppy has a strong impact on the morphology and catalytic activity [40] of polymer-modified electrodes. PMPy films were prepared using two different methods (CV and BE) and their activities toward the electrooxidation of DA were tested.

Fig. S2 in the supplementary material depicts the cyclic voltammograms of DA at bare Pt, Pt/PMPy_(BE), and Pt/PMPy_(CV). As can be seen, DA exhibit a very weak CV peak response with ΔE_p values of 333 and 227 mV at bare Pt and Pt/PMPy_(BE) electrodes, respectively. But at Pt/PMPy_(CV), the peak current increased and the peak potential shifted negatively to 536 mV. The voltammograms show a couple of reversible and well-behaved redox peaks with a ΔE_p of only 66 mV. Moreover, the difference in the electrochemical behavior between the two polymer-modified electrodes is highly manifested in the other catecholamines (E and NE), where hardly any signals were observed at Pt/PMPy_(BE) (Table 1).

This noticeable difference in the electrocatalytic activity of the two polymer films prepared under different electrochemical conditions may be explained by the surface morphology analysis (Fig. 1). The polymer film of Pt/PMPy_(BE) is compact and relatively smooth with lower surface roughness. However, Pt/PMPy_(CV) is fluffy with higher surface roughness, and that means higher surface area. Thus, the difference in electrocatalytic activity between the polymer-modified electrodes may be attributed to the larger surface area of Pt/PMPy_(CV).

Modification of PMPy with Pd nanoclusters

Characterization of Pd_{nano}-modified film electrodes

Fig. 2 shows the cyclic voltammograms of Pd_{nano}-modified electrodes tested in 0.1 M H₂SO₄. Here the voltammograms show the characteristic current features of Pd reduction (0.25 V), Pd oxide formation (0.95 V), and hydrogen adsorption and desorption (0 to -0.2 V) processes. On scanning the potential in the negative direction, Pd_{nano} are deposited on the electrode surface and the peak at approximately -0.1 V shows the reduction process of protons to hydrogen, which are adsorbed on the Pd_{nano} surface. This reduction peak confirms the hydrogen adsorption process on the Pd_{nano} surface. During the positive potential scanning process, the peak at -0.05 V appears to be due to the oxidation of hydrogen atoms. In the next step, the deposited Pd_{nano} are further oxidized to Pd²⁺ to form a Pd oxide layer (0.95 V) on the electrode surface. These peaks do not appear at Pt and Pt/PMPy_(BE) electrodes. The formed Pd oxides are further reduced on the negative-going scans, leading back to metallic Pd with hydrogen adsorption process. These observations clearly suggest the formation of Pd_{nano} and are consistent with previous reports [41].

Table 1Summary of CV results obtained at polymer and Pd_{nano}-modified polymer electrodes in 5 mM analyte/0.1 M H₂SO₄ at a scan rate of mVs⁻¹.

Compound	Pt/PMPy				Pt/PMPy _(BE) /Pd			
	BE ^a		CV ^a		I ^b		II ^b	
	E _{pa} (mV)	I _{pa} (μA)	E _{pa} (mV)	I _{pa} (μA)	E _{pa} (mV)	I _{pa} (μA)	E _{pa} (mV)	I _{pa} (μA)
Hydroquinone	496	82.6	450	47.7	456	150.1	461	241.5
Catechol	610	165.2	560	124.0	546	191.0	550	327.2
Dopamine	614	39.3	536	67.2	549	112.3	553	290.4
Methyl-L-DOPA	585	54.0	568	50.7	562	97.4	566	261.6
Epinephrine	– ^c	– ^c	567	40.3	561	84.8	564	216.8
Norepinephrine	– ^c	– ^c	571	44.3	554	89.1	557	194.1
p-Aminophenol	– ^c	– ^c	555	48.9	520	74.5	533	221.6
Acetaminophen	810	82.2	722	60.9	699	199.3	698	290.3
Ascorbic acid	– ^c	– ^c	314	53.0	295	74.8	296	120.7

Note. The deposition of Pd_{nano} on the polymer film lowers the oxidation potential (thermodynamic action) and raises the peak currents (kinetic action). For the CV results at Pt and Pd_{nano}-modified Pt electrodes, see our previous report [36].

^a Method of formation of the polymer film.

^b Method of deposition of Pd nanoclusters.

^c No signal observed.

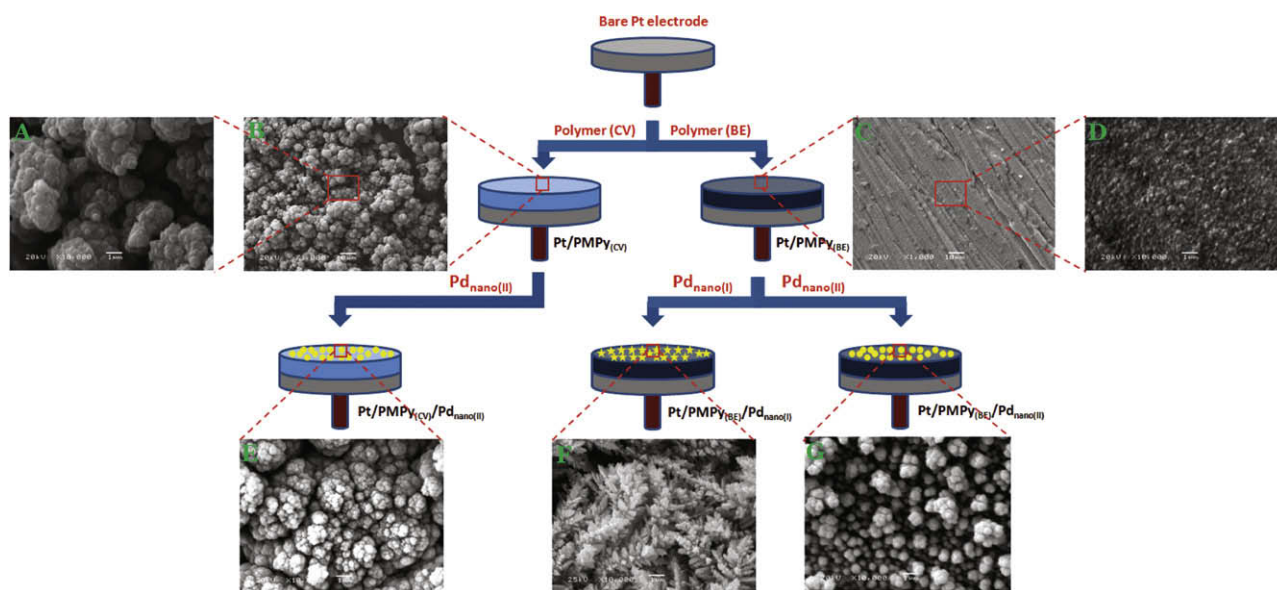


Fig. 1. Schematic showing two-step process for the modification of Pt electrode. In the first step, a polymer film is electrodeposited on Pt electrode using two electrochemical methods (BE and CV). In the second step, Pd_{nano} are deposited on the polymer film using two approaches (double potential step [I] and CV program [II]). The notation of every electrode is described. SEM micrographs for all cases are shown. See text for details. The SEM image of Pt/PMPy_(CV)/Pd_{nano(I)} is omitted because of its low electroactivity.

Effect of method of polymerization of MPy on electroactivity of PMPy/Pd_{nano} composite electrode

Fig. S3 in the supplementary material shows how changing the method of polymer film formation could affect the electroactivity of Pt/PMPy/Pd_{nano} electrodes. The results indicate that Pt/PMPy_(BE)/Pd_{nano(II)} electrode shows lower oxidation potential, higher peak currents, and lower peak separation; thus, the redox reaction of DA is thermodynamically and kinetically more favorable at this electrode when compared with Pt/PMPy_(CV)/Pd_{nano(II)} electrode, which shows very high capacitive current. Thus, although Pt/PMPy_(CV) is more electroactive when compared with Pt/PMPy_(BE), bringing Pd_{nano} to the polymer film changes this picture because the behavior of the composite electrode is a synergic phenomenon and is independent of the individual behavior of the polymer layer and Pd_{nano}. In fact, the electroactivity of PMPy/Pd_{nano} depends on the way Pd_{nano} interact with the polymer film.

Taking a look at the morphology of the PMPy/Pd_{nano} composites may help us to explain the unexpected higher electroactivity of Pt/PMPy_(BE)/Pd_{nano(II)} electrode. Scanning electron microscopy (SEM) images (Fig. 1) show that the method of polymerization affects the

size and distribution of Pd_{nano}. Pt/PMPy_(BE)/Pd_{nano(II)} exhibits spherical Pd nanoclusters with a homogeneous size distribution, whereas Pt/PMPy_(CV)/Pd_{nano(II)} exhibits smaller Pd nanoclusters but the particle sizes are not homogeneous. A further explanation of the effect of the method of formation of the polymer film on the electroactivity of PMPy/Pd_{nano} is provided in the EIS study in a later subsection.

Electrochemistry of catecholamine neurotransmitters at PMPy/Pd_{nano} electrodes with emphasis on effect of deposition of Pd nanoclusters

In this subsection, the effects of the presence of Pd_{nano} as well as the method of their deposition on the electroactivity of PMPy electrodes and the electrochemistry of catecholamine neurotransmitters are presented using CV. Fig. S4 in the supplementary material shows cyclic voltammograms for DA at PMPy films modified with Pd_{nano} electrodeposited with different methods and Pd_{nano} directly electrodeposited over Pt substrate. From Fig. S4a, it can be seen that bare Pt and Pt/PMPy_(BE) electrodes exhibit poorly defined oxidation peaks with large peak-to-peak separation at 664 and 614 mV, respectively. Moreover, the cathodic

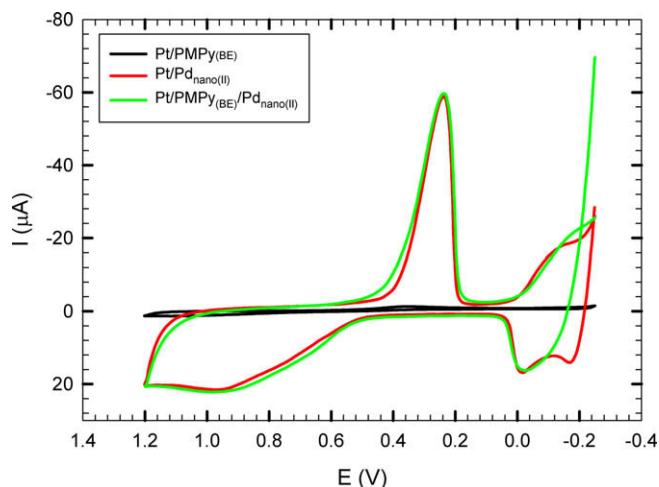


Fig. 2. Characterization of Pd_{nano}-modified electrodes. Cyclic voltammograms were obtained in 0.1 M H₂SO₄ solution at the respective electrodes with a scan rate of 20 mV s⁻¹. The voltammograms show the characteristic current features of Pd reduction (0.25 V), Pd oxide formation (0.95 V), and hydrogen adsorption and desorption (0 to -0.2 V) processes. See text for details.

peak current is much smaller than the anodic peak current. It is clear that the electron transfer kinetics of DA at the bare Pt and Pt/PMPy electrodes are sluggish [42]. On the other hand, the redox peaks at the Pt/PMPy(BE)/Pd_{nano(I)} and Pt/PMPy(BE)/Pd_{nano(II)} electrodes are reversible with the anodic peaks shifted negatively to 549 and 553 mV, respectively, and the peak currents increased significantly. Similarly, voltammograms of DA were recorded at bare Pt, Pt/Pd_{nano(I)}, and Pt/Pd_{nano(II)} (Fig. S4b). Pd_{nano}-modified Pt electrodes exhibited similar catalytic behavior for the oxidation of DA. DA demonstrated an oxidation peak at 664 mV at bare Pt, whereas the anodic peaks shifted negatively to 530 and 534 mV at Pt/Pd_{nano(I)} and Pt/Pd_{nano(II)}, respectively. Furthermore, the redox signals showed enhanced peak currents, indicating an improvement in the electrode kinetics when the Pt/Pd_{nano} electrodes are used.

Table 1 summarizes the CV results for catecholamine neurotransmitters (DA, E, and NE), precursor to catecholamines (methyl-L-DOPA), polyhydroxy phenyls (hydroquinone and catechol), *p*-aminophenol, acetaminophen, and AA at the different electrodes. At the Pd_{nano}-modified electrodes, all of the compounds showed a clear negative shift in the oxidation peak potentials accompanied by a significant increase in the anodic peak current. Thus, the remarkable enhancement in current response followed by a drop in peak potential provides clear evidence of the catalytic effect of Pd_{nano} that acts as a promoter to enhance the electrochemical reaction, considerably accelerating the rate of electron transfer. The remarkably enhanced signal at Pt/PMPy/Pd_{nano} electrodes is attributed to both of the surface-modified PMPy film and Pd_{nano}. The composite plays an important role in accelerating the electron transfer at lower potentials and increasing the oxidation current. A plot of the oxidation peak current (*I*_{pa}) versus the square root of scan rate (*v*^{1/2}) for the Pd_{nano}-modified electrodes yields a straight line in the scan rate range from 10 to 200 mV s⁻¹ (see Fig. S4 inset). Such behavior suggests that the electron transfer process at the Pd_{nano}-modified electrodes is diffusion controlled, and this is favorable for quantitative applications [43].

An SEM picture of Pt/PMPy(BE)/Pd_{nano(I)} electrode (Fig. 1F) reveals that the clusters of electrodeposited Pd exist as nanocrystallites (dendrite structures) with a preferential growth in certain crystallographic directions. This observation shows that the electrodeposition of Pd_{nano} leads to the formation of sub-microcrystallites with smaller grains (in the nano range).

EIS studies

The EIS technique is used to study the capacitance and resistance of PMPy/Pd_{nano} electrodes. Moreover, the electrochemical system studied is compared with an “equivalent circuit” that uses some of the conventional circuit elements, namely resistance, capacitance, diffusion, and induction elements. The data are represented as a relation between the impedance and the frequencies, namely the Bode plot. In all cases, the experimental data are compared with the equivalent circuit models. Thus, it is anticipated that the changes in the conditions of the experiments, as will be

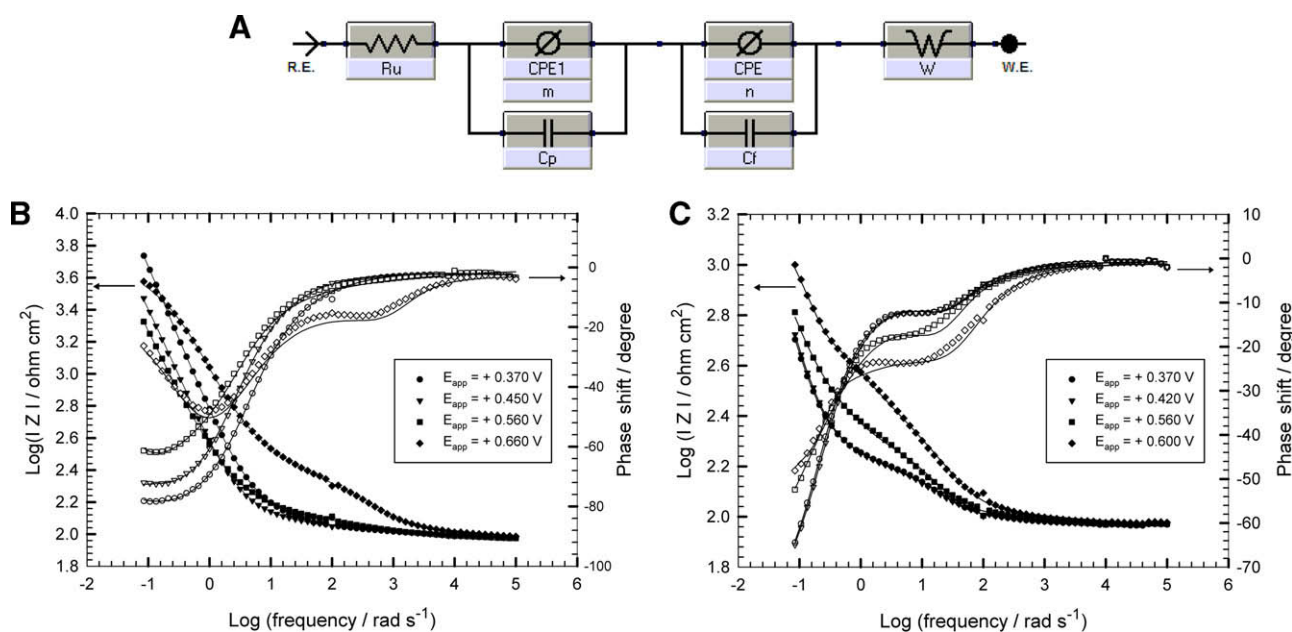


Fig. 3. Results of EIS. (A) Equivalent circuit used in the fit procedure of the impedance spectra. (B,C) Bode plot of impedance spectra for Pt/PMPy(BE)/Pd_{nano(II)} (B) and Pt/PMPy(CV)/Pd_{nano(II)} (C), all tested in 5 mM DA/0.1 M H₂SO₄. The method of preparation of the polymer film was reflected on the electrochemical impedance properties of the PMPy/Pd_{nano} composite-modified electrodes. See text for details.

described, are reflected on the electrochemical parameters. More important, the method of preparation of the polymer was reflected on the subsequent modification criteria of the film. EIS data were obtained for PMPy modified with Pd_{nano} at AC frequencies varying between 0.1 Hz and 100 kHz with an applied potential in the region corresponding to the electrolytic oxidation of DA in 0.1 M H₂SO₄. The equivalent circuit is shown in Fig. 3A. In this circuit, R_u is the solution resistance. Capacitors in EIS experiments often do not behave ideally; instead they act like a constant phase element (CPE). Therefore, CPE1 and CPE are constant phase elements, and *m* and *n* are their corresponding exponents (*m* and *n* < 1). C_p and C_f represent the capacitance of the double layer. Diffusion can create impedance known as the Warburg impedance (*W*).

Table 2 lists the best fitting values calculated from the equivalent circuit of Fig. 3A for the impedance data of Figs. 3B and C. The average error (χ^2) of the fits for the mean error of modulus was in the range of $\chi^2 = (1.5 - 3.8) \times 10^{-2}$. It is important to notice that ionic species are solvated, and their migration within the polymeric film depends on the pore size of the film. Because anionic species are the major components compensating for the charge within the polymer film [44], the contribution of solvent used that may catalytically decompose at the film/electrolyte interface is not expected except at relatively high applied potentials. Thus, polarization resistance decreases appreciably with the increase in applied potential for films formed by the CV or BE method. The change in polarization resistance is more pronounced in the case of films prepared by BE. This could be attributed to a change in morphology that is dictated mainly by the porosity of the films. The shape and compactness of each film, namely those formed by two different synthetic methods, should also contribute to the rate and mechanism of charge transfer leading to the remarkable impedance characteristics of each film.

The impedance response of the films at the low-frequency domain should be controlled by the capacitive elements. However, the deposition of the film layer, for instance, leads to a depreciated effect for applied potential for various polymer types and electrochemical method used for deposition.

PMPy shows a relatively distinct trend in the values of film capacitance (C_f) and polarization resistance (CPE) when comparing films formed by the CV and BE methods, respectively. The insulating nature of PMPy films at low applied potentials showed that the predominance of a capacitive element within the film enhances the tunneling of charge and the diffusion component due to ionic migration that can be relatively neglected. Thus, the values of the Warburg components show nearly constant values throughout the potential range studied.

It is also important to notice that for all films the charge transfer shows relatively small changes before reaching full oxidized polymer films. This indicates that whereas the ionic conductance within the film is a function of potential and its nature, the electronic conductance is not affected with the same conditions. Therefore, CPE represents mainly electronic resistance, whereas CPE1 repre-

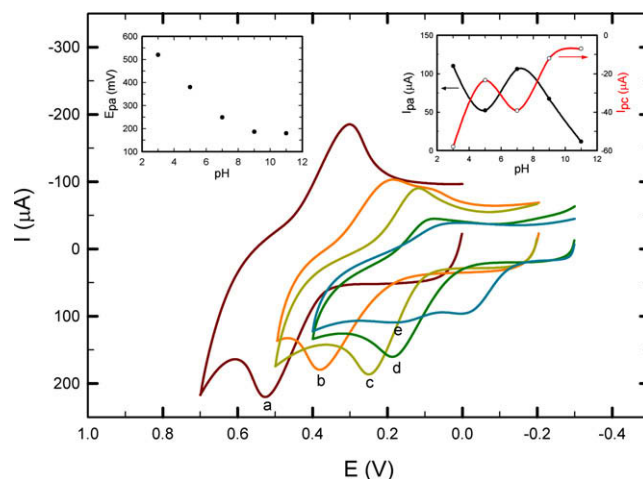


Fig. 4. Effect of pH on electrochemistry of DA. Cyclic voltammograms were obtained at the Pt/PMPy_(BE)/Pd_{nano(II)} electrode in 0.1 M PBS of different pH values: 3.0 (a), 5.0 (b), 7.0 (c), 9.0 (d), and 11.0 (e). Scan rate = 50 mV s⁻¹. Left inset: Plot of the anodic peak potential versus pH value. Right inset: Plot of the anodic peak current versus pH value. The peak potential shifted negatively with the increase of solution pH, shows Nernstian behavior over the pH range 3.0 to 7.0, and deviates at higher pH values. See text for details.

sents the predominant diffusion influence on the charge transfer process.

Effect of solution pH on electrochemistry of DA

In most cases, the solution pH is an important influence factor to the electrochemical reaction. CV was carried out to characterize the effect of solution pH on electrochemical behavior of DA at Pt/PMPy_(BE)/Pd_{nano(II)} (Fig. 4). It was found that peak potential shifted negatively with the increase of solution pH, indicating that the electrocatalytic oxidation of DA at the Pt/PMPy_(BE)/Pd_{nano(II)}-modified electrode is a pH-dependent reaction. The relationship between the anodic peak potential and the solution pH value (over the pH range 3.0–7.0) could be fit to the linear regression equation of $E_{pa}(V) = 0.7033 - 0.0609 \text{ pH}$, with a correlation coefficient of $r^2 = 0.9992$. The slope was found to be -60.9 mV/pH unit over the pH range 3.0 to 7.0, which is very close to the theoretical value of -59 mV , demonstrating that the electrode process is two-proton coupled two-electron transfer [45]. In solution, the pK_a values of DA are 8.9 (pK_{a1}) and 10.6 (pK_{a2}) [46]. A little deviation from linearity occurs at pH 9.0, indicating the deprotonation of DA at pH 9.0 so that it is no longer a two-proton, two-electron process at this point and other equilibria should be taken into account. At pH 11.0, the redox reaction of DA is no longer pH dependent because DA is completely deprotonated at this pH level. The anodic peak current (Fig. 4 right inset) decreased from pH 2.0 to 5.0 and then

Table 2
EIS fitting data corresponding to Figs. 3B and C.

Electrode	<i>E</i> (V)	<i>R</i> _u (10 ² Ω cm ²)	<i>CPE</i> 1 (F cm ⁻²)	<i>m</i>	<i>C</i> _p (10 ⁻⁶ F cm ⁻²)	<i>CPE</i> (F cm ⁻²)	<i>n</i>	<i>C</i> _f (10 ⁻⁶ F cm ⁻²)	<i>W</i> (Ω s ^{-1/2})
A	+0.370	0.5935	21,320	0.4081	324.1	59.61	0.0402	3.672	291.1
	+0.450	0.9670	3533	0.7030	340.0	66.70	0.2020	6.300	93.50
	+0.560	0.8709	2554	0.4844	624.5	129.5	0.2163	3.085	116.0
	+0.660	1.0090	623.0	0.2607	1.985	2748	0.1395	200.0	50.00
B	+0.370	0.9384	393.6	0.9102	5384	56.83	0.1205	159.2	1.479
	+0.420	0.9408	492.3	0.9000	5128	64.04	0.1500	153.4	1.378
	+0.560	0.9539	236.5	0.9000	1000	125.6	0.1790	110.6	1.119
	+0.600	0.9506	99.20	0.1500	140.7	2123	0.9000	5912	1.754

Note. A = Pt/PMPy_(BE)/Pd_{nano(II)}; B = Pt/PMPy_(CV)/Pd_{nano(II)}.

increased to pH 7.0. Above pH 7.0, the peak current decreased again.

Apparent diffusion coefficients of studied compounds at different electrodes

In this section, the dependence of the anodic peak current density on the scan rate (Fig. S4 inset) has been used for the estimation of the “apparent” diffusion coefficient, D_{app} , for the compounds studied. D_{app} values were calculated from the Randles–Sevcik equation [47]:

$$i_p = 2.69 \times 10^5 n^{3/2} A C^0 D^{1/2} \nu^{1/2}, \quad (3)$$

where i_p is the peak current density ($A\text{ cm}^{-2}$), n is the number of electrons transferred at $T = 298\text{ K}$, A is the geometrical electrode area (0.0176 cm^2), C^0 is the analyte concentration ($5 \times 10^{-6}\text{ mol cm}^{-3}$), D is the diffusion coefficient of the electroactive species ($\text{cm}^2\text{ s}^{-1}$), and ν is the scan rate (V s^{-1}).

Fig. 5 shows D_{app} values at different electrodes, namely Pt/PMPy_(BE), Pt/PMPy_(CV), Pt/PMPy_(BE)/Pd_{nano(I)}, and Pt/PMPy_(BE)/Pd_{nano(II)}. D_{app} values are between 10^{-6} and $10^{-4}\text{ cm}^2\text{ s}^{-1}$. D_{app} values at the PMPy-modified electrodes are in the range of 10^{-6} to $10^{-5}\text{ cm}^2\text{ s}^{-1}$, in good agreement with previous values reported in the literature [48,51]. In general, D_{app} values increase in the following order: Pt/PMPy_(BE) ~ Pt/PMPy_(CV) < Pt/PMPy_(BE)/Pd_{nano(I)} < Pt/PMPy_(BE)/Pd_{nano(II)}. The presence of Pd_{nano} in the polymer matrix results in an increase in the diffusion of the analyte species so that D_{app} values of some analytes at Pt/PMPy_(BE)/Pd_{nano(II)} are 100 times larger than their corresponding values at the Pt/PMPy electrodes. The values obtained at the former electrode are similar to those typically found in aqueous solution ($\sim 10^{-5}\text{ cm}^2\text{ s}^{-1}$ [49]). This is possibly due to the quick mass transfer of the analyte molecules toward electrode surface from bulk solutions and/or fast electron transfer process of electrochemical oxidation of the analyte molecule at the interface of the electrode surface and the solutions [50,51]. Furthermore, it also shows that the redox reaction of the analyte species takes place at the surface of the electrode under the control of the diffusion of the molecules from solution to the electrode surface and not within the polymer/Pd_{nano} matrix. This

might happen as a consequence of the greater number of active sites on the surface so that once the DA molecule reaches the surface of Pt/PMPy/Pd_{nano}, it oxidizes simultaneously, whereas DA diffuses on the surface of Pt/PMPy until it finds the active site for oxidation. Again, this provides additional evidence for the electrocatalytic effect of the electrodeposited Pd_{nano}.

Separation of electrochemical responses of DA, UA, and AA at Pd nanoclusters-modified PMPy electrode

It is well known that AA, DA, and UA coexist in the extracellular fluid of the central nervous system and serum [52]. Because they have similar oxidation potentials at conventional solid electrodes, separate determination of these species is a challenging problem due to their overlapped signals. Also, a large overpotential and fouling by oxidation products are additional difficulties involved in the determination of DA [53]. Therefore, Pt/PMPy_(BE)/Pd_{nano(II)} electrode was evaluated for the simultaneous voltammetric determination of AA, DA, and UA in their mixtures. Fig. 6 presents the cyclic voltammograms for the mixture of 100 μM AA, 10 μM DA, and 10 μM UA in phosphate-buffered solution (PBS, pH 7.4). As can be seen, the conventional Pt, gold (Au), and glassy carbon electrodes result in two broad and overlapped oxidation peaks. So, the peak potentials for AA, DA, and UA are indistinguishable at these conventional electrodes. Thus, it is impossible to determine the individual concentrations of these compounds from the merged voltammetric peaks. When Pt/PMPy_(BE) was used, a single broad oxidation peak appeared at approximately 230 mV. But when Pt/PMPy_(BE)/Pd_{nano(II)} was used, the overlapped voltammetric peak is resolved into three well-defined CV peaks at approximately -25, +175, and +373 mV, corresponding to the oxidation of AA, DA, and UA, respectively. An oxidation peak potential difference of 200 mV was obtained between AA and DA, and one of 198 mV was obtained between DA and UA. The observed peak separations between AA–DA and DA–UA at Pt/PMPy_(BE)/Pd_{nano(II)} are large enough for their simultaneous determination in a mixture. In addition, a substantial increase in peak currents was observed due to the improvements in the reversibility of the electron transfer pro-

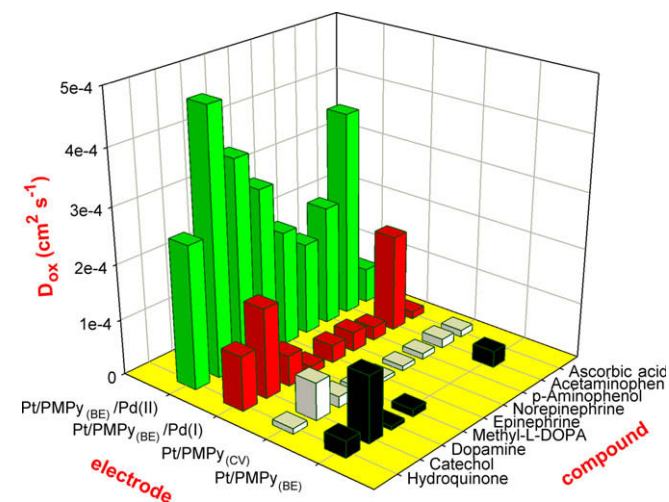


Fig. 5. Apparent diffusion coefficient (D_{app}) values for all studied compounds at the different electrodes. D_{app} was calculated from the dependence of the oxidation peak current on the scan rate according to the Randles–Sevcik equation. The deposition of Pd_{nano} into the polymer layer results in enhanced diffusion of DA. D_{app} values at Pt/PMPy_(BE)/Pd_{nano(II)} are similar to those found in aqueous solutions, indicating the fast electron transfer on its surface and/or the quick mass transfer of the analyte molecules from solution bulk toward electrode surface.

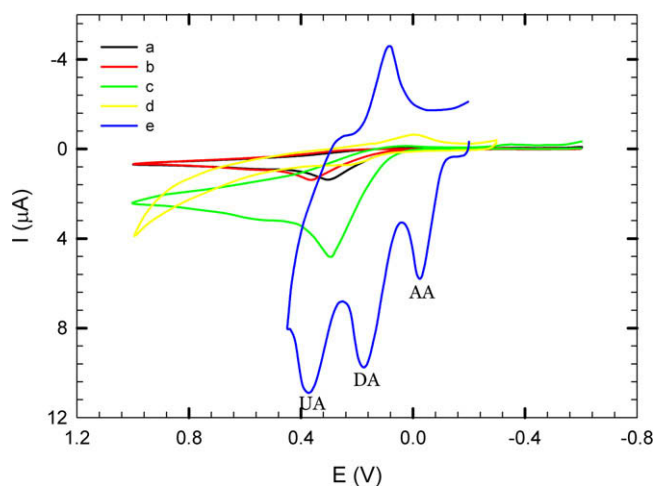


Fig. 6. Separation of electrochemical responses of AA, DA, and UA. Cyclic voltammograms of a ternary mixture of 100 μM AA, 10 μM DA, and 10 μM UA in 0.1 M PBS (pH 7.4) were obtained at Pt (a), gold (Au) (b), glassy carbon (GC) (c), Pt/PMPy_(BE) (d), and Pt/PMPy_(BE)/Pd_{nano(II)} (e). Scan rate = 50 mV s^{-1} . The conventional (Pt, Au, and GC) electrodes and Pt/PMPy_(BE) produce two broad and overlapped oxidation peaks so that the peak potentials for AA, DA, and UA are indistinguishable. However, Pt/PMPy_(BE)/Pd_{nano(II)} resolve the overlapped voltammetric peaks into three well-defined peaks corresponding to AA, DA, and UA, and the peak separations are large enough for the simultaneous determination of these analytes.

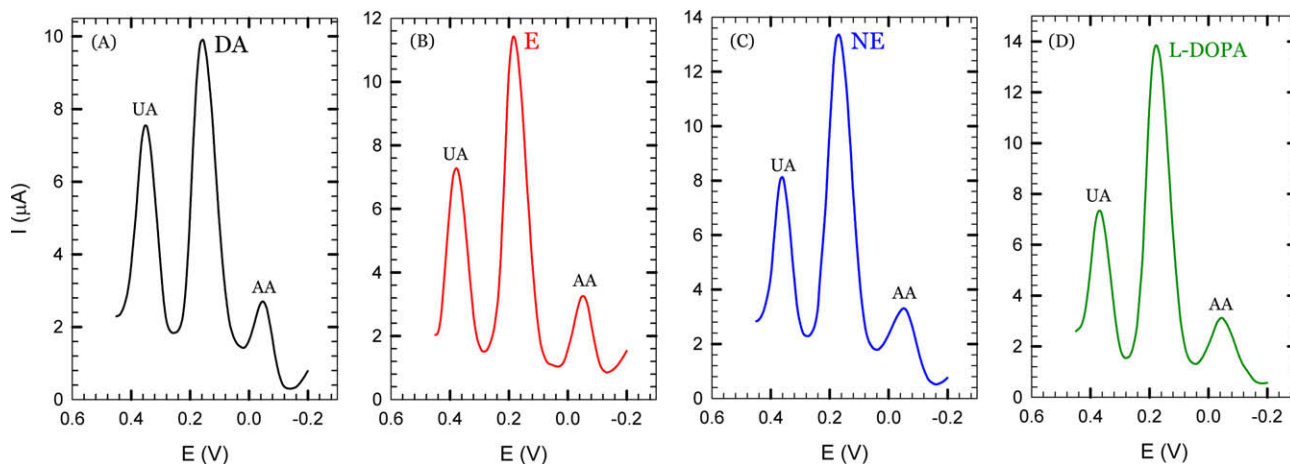


Fig. 7. Separation of the electrochemical responses of ternary mixtures of catecholamine neurotransmitters, AA, and UA. Differential pulse voltammograms were obtained at Pt/PMPy_(BE)/Pd_{nano(II)} in 0.1 M PBS (pH 7.4) for a ternary mixture of 100 μM AA, 10 μM UA, and 10 μM DA (A), 10 μM E (B), 10 μM NE (C), and 10 μM L-DOPA (D) for DPV conditions, see caption of Fig. 8. The suggested modified electrode results in three well-defined oxidation peaks and, thus, is capable of the simultaneous determination of ternary mixtures of this kind.

cesses. These observations demonstrate that PMPy/Pd_{nano} nanocomposites have high electrocatalytic activities toward the oxidation of AA, DA, and UA.

If DPV was used to value the system, three sharp and well-resolved anodic peaks at -50, 155, and 356 mV appeared for AA, DA, and UA, respectively (Fig. 7A). Thus, an oxidation peak potential difference of 205 mV was obtained between AA and DA, and one of 201 mV was obtained between DA and UA. The suggested modified electrode proves to be excellent in the simultaneous analysis of mixtures of catecholamines and their precursor, AA and UA. Differential pulse voltammograms for ternary mixtures of AA, UA, and DA (Fig. 7A), E (Fig. 7B), NE (Fig. 7C), or L-DOPA (Fig. 7D) show three well-resolved oxidation peaks. The large peak separation of the anodic peaks for mixtures of catecholamines, AA and UA, is enough to allow their simultaneous determination in a mixture solution.

Simultaneous determination of DA and UA in presence of large concentration of AA

Based on the effect of pH and considering the physiological pH condition, we selected PBS (pH 7.4) for the simultaneous determination of DA, UA, and AA at Pd_{nano}-modified PMPy electrode. Here the DPV technique was employed because it could provide a better peak resolution and current sensitivity than CV, which is most suitable for selective determination of these species in mixtures. A major problem in the electrochemical determination of DA in biological environments is the coexistence of AA in relatively high concentrations. So, it is important to investigate the electrochemical responses of DA and UA in the presence of large concentrations of AA [52]. DPV experiments were performed at Pt/PMPy_(BE)/Pd_{nano(II)} while changing the concentrations of DA and UA simultaneously at the micromolar levels and changing the concentration of AA at the millimolar level, which is typical of physiological conditions [52] (Fig. 8). The peak current of AA increases linearly with the increase of its concentration from 0.05 to 1 mM with a correlation of $r^2 = 0.9993$ and sensitivity of 0.0056 μA/μM. Similarly, the oxidation peak currents of DA and UA are also positively proportional to their concentrations in the whole working concentration range: 0.1 to 10 μM for DA and 0.5 to 20 μM for UA, with correlations of $r^2 = 0.9995$ and 0.9991 and sensitivities of 0.71 and 0.28 μA/μM for DA and UA, respectively.

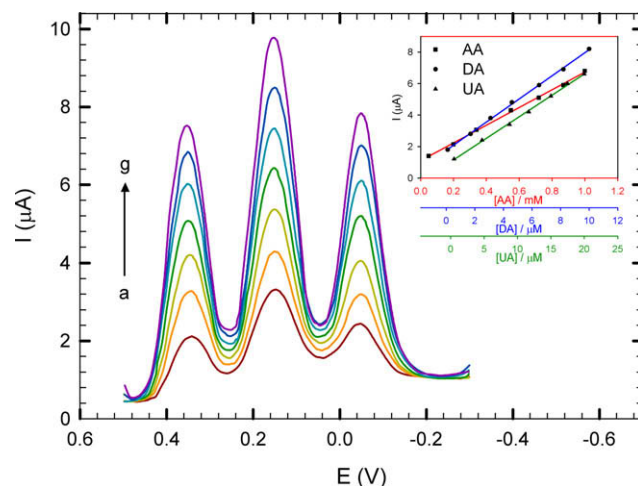


Fig. 8. Simultaneous determination of AA, DA, and UA. Differential pulse voltammograms of AA, DA, and UA were obtained at Pt/PMPy_(BE)/Pd_{nano(II)} in 0.1 M PBS (pH 7.4). Concentrations of the three compounds (a–g): AA (0.05, 0.2, 0.34, 0.55, 0.72, 0.87, and 1.0 mM); DA (0.1, 1.7, 3.2, 4.8, 6.4, 8.0, and 10.0 μM); UA (0.5, 5.0, 8.5, 11.5, 15.3, 18.0, and 20.0 μM). Inset: Corresponding calibration curves. DPV conditions: pulse amplitude = 50 mV, scan rate = 20 mV s⁻¹, sample width = 17 m s, pulse width = 50 m s, pulse period = 200 m s, and quiet time = 2 s. The peak current of AA, DA, and UA increases linearly over a concentration range typical of physiological conditions. Interestingly, the difference between peak potentials does not change with the concentration of the three species in the mixture. See text for further details.

The separations of peaks between either two-peak potentials were large enough to determine DA and UA individually and simultaneously in the presence of a high concentration of AA. Thus, no interference was observed for the determination of DA, UA, or AA by the other two coexisting species. Interestingly, the difference between peak potentials does not change with the concentration of the three species in the mixture. The detection limits (signal/noise [S/N] = 3) for AA, DA, and UA are 7 μM, 12 nM, and 27 nM, respectively. It is very interesting to notice that the detection limits of DA (S/N = 3) at Pt/PMPy_(BE)/Pd_{nano(II)} in the absence and presence of AA and UA are virtually the same (14 and 12 nM, respectively), indicating that the oxidation processes of AA, DA, and UA are independent and that the simultaneous or independent measurements of the three analytes are possible without interference. Finally, Ta-

Table 3
Comparison for simultaneous determination of AA, DA, and UA in various polymer/metal composite-based literature reports.

Electrode	Compound	pH	LDR (μM)	Sensitivity ($\mu\text{A}/\mu\text{M}$)	LOD (nM)	Real samples	Reference
CPE/CNF/Pd _{nano}	AA		50–4000	NR	15,000	NR	[54]
	DA	4.5	0.5–160	NR	200		
	UA		2–200	NR	700		
GCE/Pd _{nano}	DA in presence of 1.3 mM AA	7.0	8–88	1.014	NR	Injection solutions DHI Serum	[55]
GCE/PAT/GNP	AA	7.0	10–50	0.4	NR		
GCE/PEDOT/GNP	DA	7.4	10–50	0.22	NR	NR	[57]
	UA		0.002–0.02	200	2		
GCE/PPyox/GNP	DA in presence of AA and 5-HT	7.0	0.075–20	5.92	15	Serum	[58]
Pt/Pf/Pd _{nano}	AA in presence of ACOP		50–1000	0.0213	7130	NR	[59]
Pt/PMPy/Pd _{nano}	DA in presence of ACOP	0.1 M H ₂ SO ₄	0.5–100	0.4784	48.2	AA injection Serum Urine	This work
	AA		50–1000	0.0056	7000		
	DA	7.4	0.1–10	0.71	12		
	UA		0.5–20	0.28	27		

Note. LDR, linear dynamic range; LOD, limit of detection; NR, not reported; CPE, carbon paste electrode; CNF, carbon nanofibers; GCE, glassy carbon electrode; GNP, gold nanoparticles; PAT, poly(4-aminothiophenol); PEDOT, poly(3,4-ethylenedioxythiophene); PPyox, overoxidized polypyrrole; 5-HT, serotonin; PF, polyfuran; DHI, dopamine hydrochloride injection; ACOP, acetaminophen. The proposed electrode works over a wide LDR with high sensitivity and low detection limit and could be applied successfully in real samples.

ble 3 shows a comparison for the determination of AA, DA, and UA at Pd_{nano}-modified PMPy electrodes with various polymer/metal nanoparticles-based literature reports. The comparison shows that the suggested electrode could be used for the determination of AA, DA, and UA in various biological fluids over a wide range of concentrations with high sensitivity and low detection limits.

Interference study

As demonstrated above, such an intrinsic property of the modified electrode, Pt/PMPy_(BE)/Pd_{nano(II)}, could substantially differentiate DA, AA, and UA. Thus, the major interference from AA can be neglected. Other influences from common physiological interferences were also investigated for their effects on the determination of DA and UA, and less than $\pm 5\%$ relative error in the determination was considered. It was found that no significant interference for the detection of 10 μM DA and 10 μM UA was observed from these compounds: NaCl (5000 μM), KCl (5000 μM), CaCl₂ (1000 μM), MgCl₂ (1000 μM), glucose (10,000 μM), tryptophan (2000 μM), cysteine (2000 μM), tyrosine (2000 μM), tyramine (2000 μM), and serotonin (100 μM).

Reproducibility and stability of Pt/PMPy_(BE)/Pd_{nano(II)} electrode

The reproducibility of the Pt/PMPy_(BE)/Pd_{nano(II)} electrode system was examined by a series of 50 successive CV measurements for 100 μM DA, 100 μM E, and 100 μM UA. The relative standard deviations in peak current were found to be 3.5%, 3.0%, and 5.0%, respectively, indicating that the modified electrode had good

reproducibility and suggesting that the electrode does not undergo surface fouling during the measurements. After measurements, the modified electrode was cleaned with voltammetric cycles in PBS (pH 10.0) to eliminate the adsorption and was stored in 0.1 M PBS (pH 7.0). The modified electrode retained 92% of its initial response after 1 week.

Real sample analysis

Determination of AA in injection samples

To verify the performance of the method for analysis of AA in pharmaceutical product, the proposed electrode was applied to the determination of AA in AA injection (syrup sample) using the standard addition method. The results are shown in Table 4. The results are satisfactory, showing that the proposed method could be used efficiently for the determination of AA in injections.

Determination of UA in human urine samples

The use of the proposed method in real sample analysis was investigated by direct analysis of UA in human urine samples. To fit into the linear range of UA, all of the urine samples used for detection were diluted 400 times with 0.1 M PBS (pH 7.4). This dilution can actually help to reduce the matrix effect of real samples (see Table 4). To ascertain the correctness of the results, the samples were spiked with certain amounts of standard UA and then the total values were detected. The recovery of the spiked samples ranged between 98.88 and 100.30%, indicating that the detection procedures are free from interferences of the urine sample matrix.

Table 4
Determination of AA in injections, UA in human urine, and DA in human serum using standard addition method.

Sample type	Sample number	Content (μM)	Added (μM)	Found (μM)	Recovery (%)
AA injection	1	50	50	96.23	96.2
	2	100	100	202.3	101.2
	3	500	500	1020	102.0
Human urine	1	6.84	3	9.73	98.9
	2	6.91	3	9.62	97.1
	3	6.98	3	10.01	100.3
Human serum	1	0.1	0.1	0.19	95.0
	2	1.0	1.0	1.03	103.0
	3	5.0	5.0	10.21	102.1

Note. The recovery rates are acceptable, showing that the proposed methods could be used efficiently for the determination of these analytes in real samples.

Determination of DA in healthy human serum samples

The electrode was also applied for the recovery determination in DA hydrochloride spiking to human serum samples. All serum samples were diluted to 100 times using 0.1 M PBS (pH 7.4). The recoveries indicate that the accuracy and repeatability of the proposed voltammetric method are very good (Table 4).

Conclusions

A novel sensor has been fabricated based on the construction of PMPy polymer film further modified with Pd nanoclusters. The methods of formation of the polymer film and Pd_{nano} were found to be key factors in controlling the electroactivity of this hybrid electrode. Due to its unique properties, the PMPy/Pd_{nano} composite electrode exhibited remarkable electrocatalytic effects on the oxidation of catecholamines, AA, ACOP, and some organic compounds by increasing their oxidation peak currents and lowering their oxidation peak potentials. The most probable reason for such an increase in sensitivity is the capability of the PMPy/Pd_{nano} electrode to accelerate the rate of electron transfer of these compounds, thereby increasing the sensitivity. This was proved by CV and the diffusion coefficient measurements. Furthermore, the modified electrode can clearly distinguish ternary mixtures consisting of DA, E, NE and L-DOPA in the presence of AA and UA and, thus, is suitable for electrochemical analysis of catecholamines without the interference of AA and UA that usually exists in physiological conditions. This proposed method was applied to the determination of AA, DA, and UA in pharmaceutical product, urine, and serum samples with satisfactory results.

Acknowledgment

The authors acknowledge partial financial support from Cairo University, the office of the vice president for Graduate Studies and Research.

Appendix A. Supplementary data

Supplementary data associated with this article can be found, in the online version, at doi:10.1016/j.ab.2010.01.001.

References

- [1] B.H.C. Westerink, W. Timmerman, Do neurotransmitters sampled by brain microdialysis reflect functional release?, *Anal. Chim. Acta* 379 (1999) 263–274.
- [2] H.R. Zare, N. Rajabzadeh, N. Nasirizadeh, M.M. Ardakani, Voltammetric studies of an Oracet blue modified glassy carbon electrode and its application for the simultaneous determination of dopamine, ascorbic acid, and uric acid, *J. Electroanal. Chem.* 589 (2006) 60–69.
- [3] P. Shakkthivel, S.M. Chen, Simultaneous determination of ascorbic acid and dopamine in the presence of uric acid on ruthenium oxide modified electrode, *Biosens. Bioelectron.* 22 (2007) 1680–1687.
- [4] R.M. Wightman, L.J. May, A.C. Michael, Detection of dopamine dynamics in the brain, *Anal. Chem.* 60 (1988) 769A–779A.
- [5] O. Arrigoni, M.C. Tullio, Ascorbic acid: much more than just an antioxidant, *Biochim. Biophys. Acta* 1569 (2002) 1–9.
- [6] V.S.E. Dutt, H.A. Mottola, Determination of uric acid at the microgram level by a kinetic procedure based on a pseudo-induction period, *Anal. Chem.* 46 (1974) 1777–1781.
- [7] H.R. Zare, N. Nasirizadeh, M.M. Ardakani, Electrochemical properties of a tetrabromo-*p*-benzoquinone modified carbon paste electrode: application to the simultaneous determination of ascorbic acid, dopamine, and uric acid, *J. Electroanal. Chem.* 577 (2005) 25–33.
- [8] Z. Gao, K.S. Siow, A. Ng, Y. Zhang, Determination of ascorbic acid in a mixture of ascorbic acid and uric acid at a chemically modified electrode, *Anal. Chim. Acta* 343 (1997) 49–57.
- [9] A. Balamurugan, S.M. Chen, Poly(3,4-ethylenedioxythiophene-co-(5-amino-2-naphthalenesulfonic acid)) (PEDOT-PANS) film modified glassy carbon electrode for selective detection of dopamine in the presence of ascorbic acid and uric acid, *Anal. Chim. Acta* 596 (2007) 92–98.
- [10] L. Zhang, X.E. Jiang, Attachment of gold nanoparticles to glassy carbon electrode and its application for the voltammetric resolution of ascorbic acid and dopamine, *J. Electroanal. Chem.* 583 (2005) 292–299.
- [11] C.R. Raj, K. Tokuda, T. Ohsaka, Electroanalytical applications of cationic self-assembled monolayers: square-wave voltammetric determination of dopamine and ascorbate, *Bioelectrochemistry* 53 (2001) 183–191.
- [12] S.B. Adeloju, G.G. Wallace, Conducting polymers and the bioanalytical sciences: new tools for biomolecular communications, *Analyst* 121 (1996) 699–703.
- [13] D.H. Han, H.J. Lee, S.M. Park, Electrochemistry of conductive polymers: XXXV. Electrical and morphological characteristics of polypyrrole films prepared in aqueous medium studied by current sensing atomic force microscopy, *Electrochim. Acta* 50 (2005) 3085–3092.
- [14] U. Johanson, A. Marandi, T. Tamm, J. Tamm, Comparative study of the behavior of anions in polypyrrole films, *Electrochim. Acta* 50 (2005) 1523–1528.
- [15] E. Krivan, G. Peintler, C. Visy, Matrix rank analysis of spectral studies on the electropolymerization and discharge process of conducting polypyrrole/dodecyl sulfate films, *Electrochim. Acta* 50 (2005) 1529–1535.
- [16] M.M. Chehimi, M.L. Abel, C. Perruchot, M. Delamar, S.F. Lascelles, S.P. Armes, The determination of the surface energy of conducting polymers by inverse gas chromatography at infinite dilution, *Synth. Met.* 104 (1999) 51–59.
- [17] A. Azioune, F. Siroti, J. Tanguy, M. Jouini, M.M. Chehimi, B. Miksa, S. Slomkowski, Interactions and conformational changes of human serum albumin at the surface of electrochemically synthesized thin polypyrrole films, *Electrochim. Acta* 50 (2005) 1661–1667.
- [18] B. Saoudi, C. Despas, M.M. Chehimi, N. Jammul, M. Delamar, J. Bessiere, A. Walcarius, Study of DNA adsorption on polypyrrole: interest of dielectric monitoring, *Sens. Actuat. B* 62 (2000) 35–42.
- [19] V.G. Khomenko, V.Z. Barsukov, A.S. Katashinskii, The catalytic activity of conducting polymers toward oxygen reduction, *Electrochim. Acta* 50 (2005) 1675–1683.
- [20] N.T.L. Hien, B. Garcia, A. Pailleret, C. Deslouis, Role of doping ions in the corrosion protection of iron by polypyrrole films, *Electrochim. Acta* 50 (2005) 1747–1755.
- [21] A. Ramanaviciene, A. Ramanavicius, in: D.W. Thomas (Ed.), *Advanced Biomaterials for Medical Applications*, Kluwer Academic, Dordrecht, Netherlands, 2004, p. 111.
- [22] A. Ramanavicius, K. Habermuler, V. Laurinavicius, E. Csoregi, W. Shuhmann, Polypyrrole-entrapped quinoxaline alcohol dehydrogenase: Evidence for direct electron transfer via conducting-polymer chains, *Anal. Chem.* 71 (1999) 3581–3586.
- [23] A. Ramanaviciene, A. Ramanavicius, Application of polypyrrole for the creation of immunosensors, *Crit. Rev. Anal. Chem.* 32 (2002) 245–252.
- [24] A. Ramanaviciene, A. Ramanavicius, Pulsed amperometric detection of DNA with an ssDNA/polypyrrole-modified electrode, *Anal. Bioanal. Chem.* 379 (2004) 287–293.
- [25] A. Ramanaviciene, A. Ramanavicius, Molecularly imprinted polypyrrole-based synthetic receptor for direct detection of bovine leukemia virus glycoproteins, *Biosens. Bioelectron.* 20 (2004) 1076–1082.
- [26] A. Malinauskas, J. Malinauskiene, A. Ramanavicius, Conducting polymer-based nanostructured materials: electrochemical aspects, *Nanotechnology* 16 (2005) R51–R62.
- [27] H.L. Schmidt, F. Gutberlet, W. Schuhmann, New principles of amperometric enzyme electrodes and of reagentless oxidoreductase biosensors, *Sens. Actuat. B* 13 (1993) 366–371.
- [28] J.J. Kim, T. Ameniya, D.A. Tryk, K. Hashimoto, A. Fujishima, Charge transport processes in electrochemically deposited polypyrrole and poly(*N*-methylpyrrole) thin films, *J. Electroanal. Chem.* 416 (1996) 113–119.
- [29] A.M. Bitter, Clusters on soft metal surfaces, *Surf. Sci. Rep.* 61 (2006) 383–428.
- [30] S. Dominguez-Dominguez, J. Arias-Pardilla, A. Berenguer-Murcia, E. Morallon, D. Cazorla-Amoros, Electrochemical deposition of platinum nanoparticles on different carbon supports and conducting polymers, *J. Appl. Electrochem.* 38 (2008) 259–268.
- [31] H. Tang, J. Chen, L. Nie, D. Liu, W. Deng, Y. Kuang, S. Yao, High dispersion and electrocatalytic properties of platinum nanoparticles on graphitic carbon nanofibers (GCNFs), *J. Colloid Interface Sci.* 269 (2004) 26–31.
- [32] Z. He, J. Chen, D. Liu, H. Tang, W. Deng, Y. Kuang, Deposition and electrocatalytic properties of platinum nanoparticles on carbon nanotubes for methanol electrooxidation, *Mater. Chem. Phys.* 85 (2004) 396–401.
- [33] J.V. Zoval, J. Lee, S. Gorer, R.M. Penner, Electrochemical preparation of platinum nanocrystallites with size selectivity on basal plane oriented graphite surfaces, *J. Phys. Chem. B* 102 (1998) 1166–1175.
- [34] (a) A.P. O'Mullane, S.E. Dale, T.M. Day, N.R. Wilson, J.V. Macpherson, P.R. Unwin, Formation of polyaniline/Pt nanoparticle composite films and their electrocatalytic properties, *J. Solid State Electr.* 10 (2006) 792–807; (b) B.C. Sih, M.O. Wolf, Metal nanoparticle-conjugated polymer nanocomposites, *Chem. Commun.* (2005) 3375–3384.
- [35] N.F. Atta, I. Marawi, K.L. Petticrew, H. Zimmer, H.B. Mark Jr., A. Galal, Electrochemistry and detection of some organic and biological molecules at conducting polymer electrode: III. Evidence of the electrocatalytic effect of the heteroatom of the poly(heteroarylene) at the electrode/electrolyte interface, *J. Electroanal. Chem.* 408 (1996) 47–52.
- [36] N.F. Atta, M.F. El-Kady, Poly(3-methylthiophene)/palladium sub-micro-modified sensor electrode: II. Voltammetric and EIS studies, and analysis of catecholamine neurotransmitters, ascorbic acid, and acetaminophen, *Talanta* 79 (2009) 639–647.

- [37] E. Laviron, General expression of the linear potential sweep voltammogram in the case of diffusionless electrochemical systems, *J. Electroanal. Chem.* 101 (1979) 19–28.
- [38] S. Sadki, P. Scholtland, N. Brodie, G. Sabonraud, The mechanisms of pyrrole electropolymerization, *Chem. Soc. Rev.* 29 (2000) 283–293.
- [39] R.J. Waltman, J. Bargon, A.F. Diaz, Substituent effects in the electropolymerization of aromatic heterocyclic compounds, *J. Phys. Chem.* 88 (1984) 4343–4346.
- [40] A. Ramanavicius, A. Ramanaviciene, A. Malinauskas, Electrochemical sensors based on conducting polymer–polypyrrole, *Electrochim. Acta* 51 (2006) 6025–6037.
- [41] (a) P. Santhosh, K.M. Manesh, S. Uthayakumar, S. Komathi, A.I. Gopalan, K.-P. Lee, Fabrication of enzymatic glucose biosensor based on palladium nanoparticles dispersed onto poly(3,4-ethylenedioxythiophene) nanofibers, *Bioelectrochemistry* 75 (2009) 61–66;
(b) V.C. Diculescu, A.M.C. Paquim, O. Corduneanu, A.M.O. Brett, Palladium nanoparticles and nanowires deposited electrochemically: AFM and electrochemical characterization, *J. Solid State Electr.* 11 (2007) 887–898.
- [42] A. Salimi, H. Mam-Khezri, R. Hallaj, Simultaneous determination of ascorbic acid, uric acid, and neurotransmitters with a carbon ceramic electrode prepared by sol–gel technique, *Talanta* 70 (2006) 823–832.
- [43] A. Kiszka, *Electrochemistry II*, Technical Scientific, Warsaw, Poland, 2001.
- [44] H. Sakai, R. Baba, K. Hashimoto, A. Fujishima, A. Heller, Local detection of photoelectrochemically produced H₂O₂ with a “wired” horseradish peroxidase microsensor, *J. Phys. Chem.* 99 (1995) 11896–11900.
- [45] L.M. Niu, N.B. Li, W.J. Kang, Electrochemical behavior of uric acid at a penicillamine self-assembled gold electrode, *Microchim. Acta* 159 (2007) 57–63.
- [46] D.R. Lide (Ed.), *Handbook of Chemistry and Physics*, 84th ed., CRC Press, Boca Raton, FL, 2004.
- [47] J. Wang, *Analytical Electrochemistry*, third ed., John Wiley, Hoboken, NJ, 2006, p. 32.
- [48] X. Wang, N. Yang, Q. Wan, X. Wang, Catalytic capability of poly(malachite green) films based electrochemical sensor for oxidation of dopamine, *Sens. Actuat. B* 128 (2007) 83–90.
- [49] B.J. Venton, K.P. Troyer, R.M. Wightman, Response times of carbon fiber microelectrodes to dynamic changes in catecholamine concentration, *Anal. Chem.* 74 (2002) 539–546.
- [50] Q. Wan, N. Yang, X. Zou, H. Zhang, B. Xu, Voltammetric behavior of vitamin B2 on the gold electrode modified with a self-assembled monolayer of L-cysteine and its application for the determination of vitamin B2 using linear sweep stripping voltammetry, *Talanta* 55 (2002) 459–467.
- [51] V.S. Vasantha, S.-M. Chen, Electrocatalysis and simultaneous detection of dopamine and ascorbic acid using poly(3, 4-ethylenedioxy)thiophene film modified electrodes, *J. Electroanal. Chem.* 592 (2006) 77–87.
- [52] A.J. Downard, A.D. Roddick, A.M. Bond, Covalent modification of carbon electrodes for voltammetric differentiation of dopamine and ascorbic acid, *Anal. Chim. Acta* 317 (1995) 303–310.
- [53] V.S. Ijleri, P.V. Jaiswal, A.K. Srivastava, Chemically modified electrodes based on macrocyclic compounds for determination of Vitamin C by electrocatalytic oxidation, *Anal. Chim. Acta* 439 (2001) 291.
- [54] J. Huang, Y. Liu, H. Hou, T. You, Simultaneous electrochemical determination of dopamine, uric acid, and ascorbic acid using palladium nanoparticle-loaded carbon nanofibers modified electrode, *Biosens. Bioelectron.* 24 (2008) 632–637.
- [55] S. Thiagarajan, R.-F. Yang, S.-M. Chen, Palladium nanoparticles modified electrode for the selective detection of catecholamine neurotransmitters in presence of ascorbic acid, *Bioelectrochemistry* 75 (2009) 163–169.
- [56] A.I. Gopalan, K.-P. Lee, K.M. Manesh, P. Santhosh, J.H. Kim, J.S. Kang, Electrochemical determination of dopamine and ascorbic acid at a novel gold nanoparticles distributed poly(4-aminothiophenol) modified electrode, *Talanta* 71 (2007) 1774–1781.
- [57] J. Mathiyarasu, S. Senthilkumar, K.L.N. Phani, V. Yegnaraman, PEDOT–Au nanocomposite film for electrochemical sensing, *Mater. Lett.* 62 (2008) 571–573.
- [58] J. Li, X. Lin, Simultaneous determination of dopamine and serotonin on gold nanocluster/overoxidized–polypyrrole composite modified glassy carbon electrode, *Sens. Actuat. B* 124 (2007) 486–493.
- [59] N.F. Atta, M.F. El-Kady, A. Galal, Palladium nanoclusters-coated polyfuran as a novel sensor for catecholamine neurotransmitters and paracetamol, *Sens. Actuat. B* 141 (2009) 566–574.